

This article appeared in a journal published by Elsevier. The attached copy is furnished to the author for internal non-commercial research and education use, including for instruction at the authors institution and sharing with colleagues.

Other uses, including reproduction and distribution, or selling or licensing copies, or posting to personal, institutional or third party websites are prohibited.

In most cases authors are permitted to post their version of the article (e.g. in Word or Tex form) to their personal website or institutional repository. Authors requiring further information regarding Elsevier's archiving and manuscript policies are encouraged to visit:

<http://www.elsevier.com/copyright>



Contents lists available at ScienceDirect

# Nuclear Instruments and Methods in Physics Research A

journal homepage: [www.elsevier.com/locate/nima](http://www.elsevier.com/locate/nima)

## Performance simulation of a detector for 4th generation photon sources: The AGIPD<sup>☆</sup>

G. Potdevin<sup>\*</sup>, U. Trunk, H. Graafsma

Detector Systems, DESY, Notkestr. 85, 22607 Hamburg, Germany

For the AGIPD Consortium

### ARTICLE INFO

Available online 3 April 2009

Keywords:

XFEL  
Hybrid pixel detectors  
Simulation  
AGIPD

### ABSTRACT

Future 4th generation photon sources, such as the European XFEL based in Hamburg, will deliver around  $10^{12}$  X-ray photons in less than 100 fs with full lateral coherence. These new sources will offer unprecedented possibilities in photon science.

The high peak brilliance, combined with a 5 MHz repetition rate poses very high demands for the 2D detectors. In order to provide appropriate detectors during XFEL startup, three dedicated development projects have been initiated, one of them being the Adaptive Gain Integrating Pixel Detector (AGIPD) project which is a collaborative effort between DESY, PSI, University of Bonn, and University of Hamburg. An essential part of the AGIPD project is the development of a simulation tool for the complete detection system. The simulation tool as well as preliminary simulations of the detector characteristics is presented.

© 2009 Elsevier B.V. All rights reserved.

## 1. The European XFEL project

The European XFEL is a project aiming at the construction of a large scale X-ray Free Electron Laser facility in Hamburg, Germany. This 4th generation photon source, based on the principle of Self-Amplification of Spontaneous Emission (SASE), will produce *extremely short coherent* photon pulses (100 fs) with wavelengths down to 0.1 nm and will generate an unprecedented peak brilliance of  $10^{33}$  photons/(s mrad<sup>2</sup> mm<sup>2</sup> 0.1% BW).

The machine will be composed of a 2.1 km long LINAC accelerating electrons up to an energy of 17.5 GeV and feed five photon beamlines. The time structure of the produced photon bunches is non-regular (see Fig. 1) and thus of particular importance for the detector developments. The 100 fs long photon pulses are produced at a repetition rate of 5 MHz in 0.6 ms long pulse trains (~3000 pulses/train) and pulse trains are separated by a 99.4 ms time gap (as the superconducting accelerator has to cool down). Details on the technical aspects as well as on the scientific case and applications can be found in the Technical Design Report (TDR [1]). Complementary information can be found on the XFEL project's website [2].

## 2. The AGIPD detector concepts

The *Adaptive Gain Integrating Pixel Detector* (AGIPD) project<sup>1</sup> is a collaboration between DESY, PSI, University of Bonn, and University of Hamburg, established to develop and construct a detector with 1 million pixels, of  $200 \times 200 \mu\text{m}^2$ , based on the *hybrid pixel technology* (see Helmut Spieler textbook [3]). Each pixel will contain an adaptive slope integrator needed to cover the full dynamic range from single photon detection up to  $10^4$  12 keV photons per 100 fs pulse, as well as an analog pipeline for frame storage at the 5 MHz repetition rate (Fig. 2). Precautions will also be taken to make the detector sufficiently radiation hard, as the total integrated lifetime dose could exceed 1 GGy. A single ASIC will contain  $64 \times 64$  pixels and be three side buttable,  $4 \times 2$  ASICs will be bump-bonded to a monolithic 500 or 700  $\mu\text{m}$  thick silicon sensor to form a module, and  $(4 \times 8)$  modules will be assembled to form the complete  $1 \text{ K} \times 1 \text{ K}$  pixel detector (see Fig. 3). In order to allow the direct beam as well as the forward scattered sample signal to pass without damaging the detector, a hole is present at the center of the detector. The readout of the analog pipeline and digital conversion will be done during the 99.4 ms time gap between bunch trains. As many pictures as possible, at least several hundred, will be stored in the ASIC during the bunch train. The exact number will be determined as a compromise between

<sup>☆</sup> <http://hasylab.desy.de/science/developments/detectors/AGIPD/>

<sup>\*</sup> Corresponding author.

E-mail address: [guillaume.potdevin@desy.de](mailto:guillaume.potdevin@desy.de) (G. Potdevin).

<sup>1</sup> Formerly called HPAD.

various conflicting parameters like noise versus number of storage capacitors.

**3. The simulation of the detector performances**

In order to identify critical components, to determine the implications of necessary compromises, and to provide the future users of the XFEL facility with an improved knowledge of the detector's performances, a project of simulation of both the scientific experiments and the detector response was started. In the following only the simulation of the detector response will be described. The simulation tool *HORUS* (for Hpads Overall Response fUnction Simulator-written in IDL) is based on a modular and pluggable structure allowing simulated effects to be suppressed or modified independently of each other. The code structure is schematically represented in Fig. 4. The program takes an intensity distribution impinging on its entrance window as its starting point. The intensity distribution can be derived from simulations or extrapolated from experimental data obtained at 3rd generation storage rings. The dead areas (space in-between modules, central hole) and special pixels (the pixels between the

ASICS have double or quadruple sizes) are first taken into account. Subsequently the response to each single photon is determined. In order to increase the spatial resolution in the simulation the intensity distribution across a pixel can be estimated by fitting a linear density function to the intensities of the pixel and the adjacent neighbours. It is also possible to use highly oversampled data (the limitation is the computer's memory). The depth of absorption and parallax shift are determined statistically respecting the material's mass absorption coefficients. All the photon energy is assumed to be deposited locally upon photon absorption, and converted into electron-hole pairs, properly taking statistical fluctuations and the fano factor into account. The spreading of the electron cloud during its drift to the readout electrodes is simulated by a Gaussian with a variance  $\sigma = \sqrt{2Dt}$  (theoretical formula as found in Knoll and Spieler [4,3]), where  $D$  is the diffusion coefficient and  $t$  the collection time (Fig. 5). In this

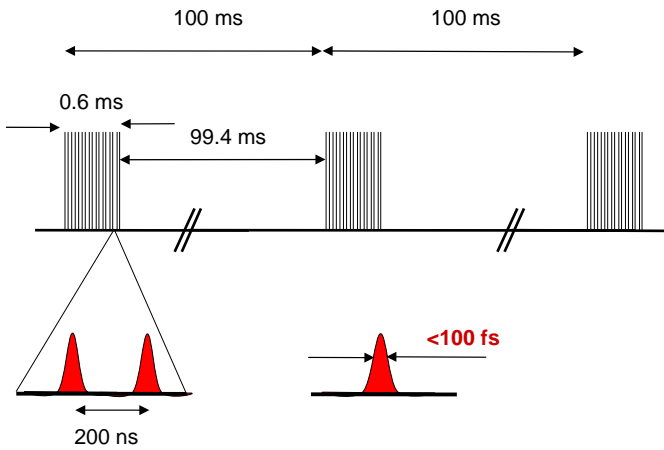


Fig. 1. The photon bunches time structure.

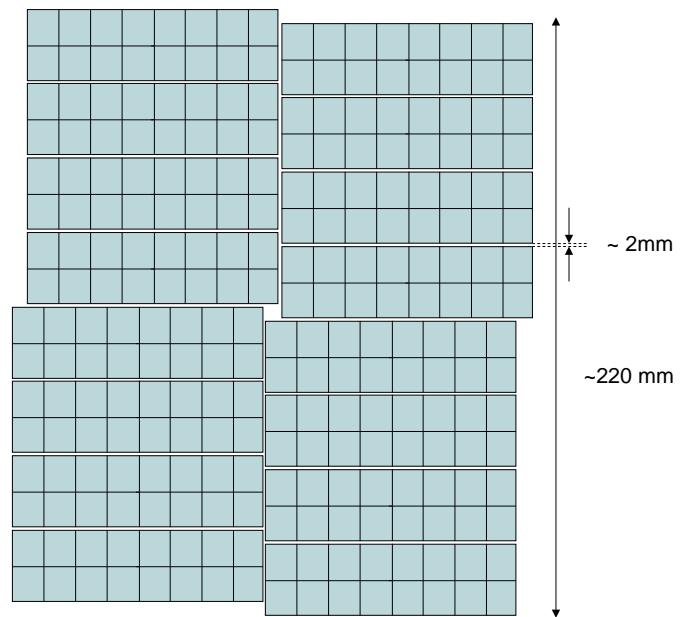


Fig. 3. The AGIPD layout.

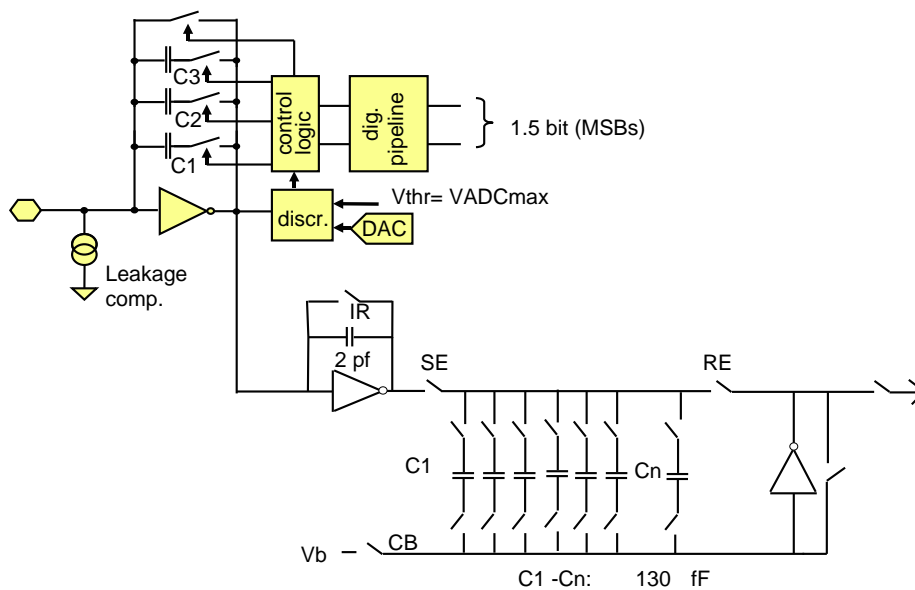


Fig. 2. The front end electronics layout.

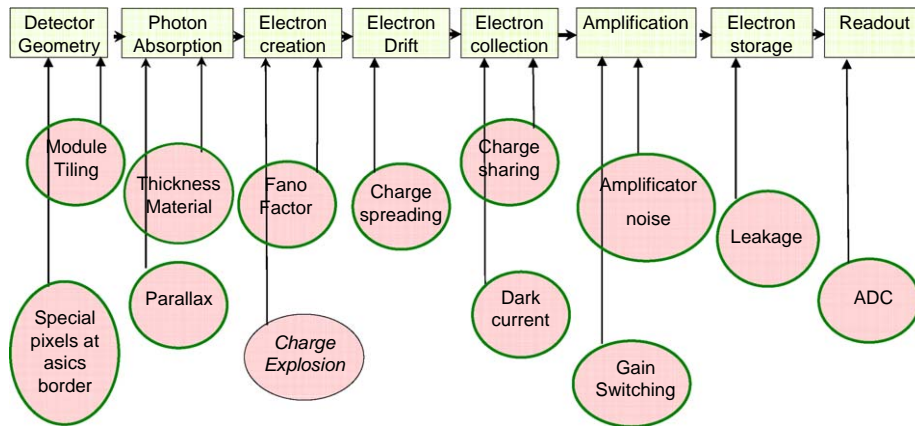


Fig. 4. The HORUS code structure.

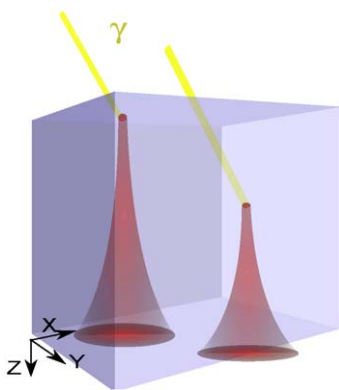


Fig. 5. Photon absorption and electron cloud spreading in the sensor.

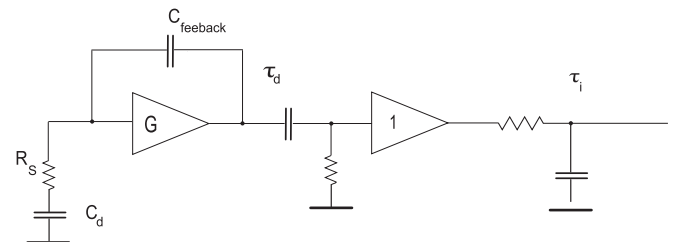


Fig. 6. Equivalent noise model for the front end electronics.

model, the variance is assumed to be  $\sigma(z) = 0.38\sqrt{z}[\sqrt{\mu\text{m}}]$  with  $z$  the distance to the collecting electrodes in  $\mu$ . This value was fitted to the result of Fowler et al. [5]. For example, a 500  $\mu\text{m}$  long drift results in a spreading of variance  $\sigma = 8.4\sqrt{\mu\text{m}}$ .

The model does not yet take into account the possible anomalous effects that might occur at very high local X-ray intensities, which lead to charge concentrations approaching or exceeding the dopant/intrinsic charge density which in turn give rise to a electron–hole plasma. The reaction of silicon detectors to such high levels of electrons and holes is the topic of a separate theoretical study and the results will eventually be implemented into the code. The model for the front end electronics is a charge sensitive amplifier followed by a basic CR-RC shaper (the actual circuit which will be implemented will be more complicated, but has the same function), the equivalent model is depicted in Fig. 6 (details can be found in Spieler [3]). The noise contribution of the gain switching system is not yet implemented into the simulation code. Currently the analog pipeline loss of charge is modeled with the form  $\delta q = aq + b$ , where a constant loss of charge,  $b$ , is assumed when the switches are operated plus a capacitor leakage proportional to the stored charge  $q$  given by the factor  $a$  (a worst case of 100 ms long storage is taken). The (commercially available) analog to digital converter (resolution of 14 bit) is believed to have a minor contribution to the overall noise and only its documented characteristics are included in the code.

In general, the parameters used in the simulation are either obtained from comparison with similar systems like the Pilatus detector, which was developed at PSI (input pre-amplifier capacitance, parallel and series preamplifier resistances—reference publication is from Broennimman et al. [6]), or from simulation using

the foundry-provided tools and models (parallel and series amplifier noise, transistor transconductance, amplifier gain). Precise measurements of the key components will be done in the near future using specially prepared test structures and an experimental setup.

### 3.1. Preliminary results

The simulation tool is used to evaluate the detector's performance (spatial resolution, intrinsic noise contribution), to help decide on compromises, and to prepare future XFEL experiments. Fig. 7 shows the simulated detector response to an intense photon pulse (three pixels wide) incident at the center and the border of the detector, for two sensor thicknesses (500 and 700  $\mu\text{m}$ ). The simulation corresponds to a typical XFEL experiment (coherently diffracted beam, distance sample-detector  $\sim 30$  cm).

One of the first decisions to be taken concerns the target sensor thickness. In order to choose between those two thicknesses, the modulation transfer function (MTF) and the expected noise were evaluated both at the center and at the border of the detector in typical experimental conditions. The MTF measurements are depicted in Fig. 8. In these simulations, the effect of the polarization is not taken into account.

The noise was also evaluated in both cases as the sensor thickness impacts the overall noise characteristics. The first noise parameter changing with the sensor thickness  $d$  is the input capacitance. The capacitance  $C$  per unit area  $A$  is  $C/A = \epsilon/w$ , where  $\epsilon$  the silicon dielectric constant and  $w$  the depleted thickness (see Spieler as well as Rossi [3,7]). As the sensor will be fully depleted,  $C/A \approx \epsilon/d$ . The second parameter is the sensor shot noise, which increases with the sensor volume. It appears that the noise remains the same for both thicknesses (the simulation tool predicts an equivalent noise charge of 160 electrons) as the contribution of the sensor capacitance to the

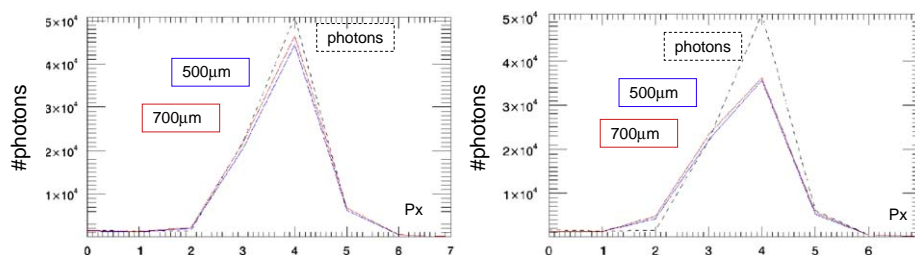


Fig. 7. Profile of the detector response to an input photon bragg peak (dashed line) at the center (left figure) and border (right figure) of the detector, for 500 and 700  $\mu\text{m}$  thick sensors.

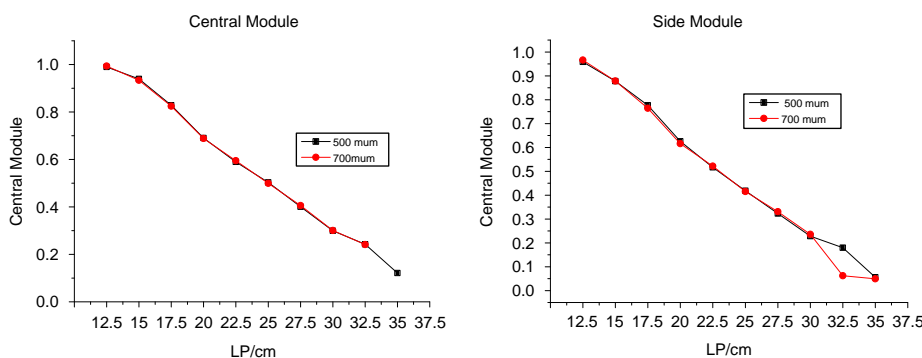


Fig. 8. The modulation transfer function for central (left figure) and side (right figure) modules for 500 and 700  $\mu\text{m}$  thick silicon sensors. In both cases, measurements do not show any difference in resolution.

overall input amplifier capacitance is negligible and as the sensor shot noise is negligible with respect to the other sources of noise. The conclusion of this study is that the increased sensor thickness does not translate into notably worse MTF, nor noise, while it enables an appreciable gain in stopping power (96% versus 90% for 12 keV photons). This increased stopping power is extremely important as the integrated dose on the detector is expected to be high (up to 1 GGy), and the use of the thicker sensor reduces the integrated dose seen by the ASIC by 60% when compared to the thinner sensor.

#### 4. Summary and future

A complete simulation tool of the XFEL dedicated AGIPD pixel detector is being developed by the AGIPD consortium. This tool is already used to identify critical components in the AGIPD, to help deciding on compromises, and will be used to help preparing XFEL experiments to be carried out at the European XFEL with the AGIPD detector. The tool was already used to make some critical choices concerning the AGIPD features (sensor thickness, pixel size), and will soon be used to evaluate the detector's response to simulated XFEL experiments (single object imaging).

In the future, it is planned to improve the simulation tool by a more careful evaluation of each of the simulation parameters and made available to others. In particular measurements of specially prepared test structures will be made; the possible effect of the analog pipeline on the overall detector performances will also be studied in detail.

#### Acknowledgments

The authors would like to thank the European XFEL for the funding of this project, and the AGIPD Collaboration members for many fruitful discussions.

#### References

- [1] M. Altarelli, et al., European Xray free electron laser technical design report, Technical Report, The European XFEL, 2007.
- [2] European XFEL website, (<http://www.xfel.eu/>).
- [3] H. Spieler, Semiconductor Detector Systems, Oxford Science Publications, 2008.
- [4] G.F. Knoll, Radiation Detection and Measurement, Wiley, New York, 2000.
- [5] R.F. Fowler, et al., Nucl. Instr. and Meth. A 477 (2002) 226.
- [6] Ch. Broennimann, et al., J. Synchrotron Rad. 13 (2006) 120.
- [7] L. Rossi, et al., Pixel Detectors, Springer, Berlin, 2006.